

REVIEW

Open Access



# Intelligent compaction methods and quality control

Yangping Yao<sup>1</sup> and Erbo Song<sup>1\*</sup>

## Abstract

Ensuring high-quality fill compaction is crucial for the stability and longevity of infrastructures and affects the sustainability of urban infrastructure networks. The purpose of this paper is to provide a refined analysis and insight understanding of the current practice, limitations, challenges, and future development trends of compaction methods from the perspective of the development stage. This paper offers a comprehensive overview of the evolution of compaction methods and classifies compaction quality control methods into four groups through quantitative analysis of literature: traditional compaction methods, digital compaction methods, automated compaction methods, and intelligent compaction methods. Each method's properties and issues are succinctly stated. Then, the research on three key issues in intelligent compaction including compaction quality evaluation algorithms, dynamic optimal path planning, and implementation of unmanned technology is summarized. Currently, the field of intelligent compaction is far from mature, a few challenges and limitations need further investigation: coupling problems of multiple indicators in intelligent evaluation algorithms, unmanned roller groups collaborative control problems, and intelligent decision-making and optimization problems of multi-vehicle compaction paths. This review serves as a valuable reference for systematically understanding the development of compaction methods.

**Keywords** Traditional compaction, Digital compaction, Automated compaction, Intelligent compaction, Compaction quality evaluation algorithm, Dynamic optimal path planning, Unmanned driving technology

## 1 Introduction

The strength and resistance to plastic deformation of the soil-filling are significantly increased under compaction. The stability and safety of infrastructure like roads [1–3], airports [4–8], dams [9–12], and railways [13–15] rely on the roadbed or subgrade's ability to resist deformation. Therefore, the compaction quality of the filling needs to be strictly controlled to ensure the longevity and stability of these infrastructures and prevent potential consequences. Inadequate compaction of airport filling can lead to serious consequences such as road surface fractures, deformations, and uneven settlement. For example,

uneven settlement on the runway of Lijiang Airport impacts safe operation, as shown in Fig. 1. In the meantime, improving the quality of road construction plays a crucial role in the development of a more sustainable and cost-effective urban infrastructure network in the transport sector.

Traditional compaction methods depend on active supervision during construction and random sampling tests after completion to evaluate the compaction quality of the filling, but they have obvious limitations, such as: (1) The conventional management approach is outdated. The human factor is a major influence on the manual supervision and management mode, which is prone to misjudgment of the number of compaction passes, and poor precision in controlling compaction quality can result in under-compaction, miss-compaction, and over-compaction in the construction area [16]. (2) The locations for routine sampling may not be representative

\*Correspondence:

Erbo Song  
by1713119@buaa.edu.cn

<sup>1</sup> School of Transportation Science and Engineering, Beihang University, Beijing, China





**Fig. 1** Photo of uneven settlement happened on the Lijiang Airport runway

due to there are only a limited number of random sampling locations on the site, which can hardly represent the compaction quality of the entire construction area. Moreover, sampling tests are more applicable for uniform samples. When the properties of fillings are distributed discretely, the distribution of the sampling test results do not follow a normal distribution, making it more challenging to use the results as the foundation for judging the compaction quality of the entire construction area [17]. (3) Inefficient and expensive. Some detection methods are destructive, which would damage the road's surface. Others may require professional workers to operate with a long time span and are prone to delay the construction progress. Therefore, these inefficient, high-cost detection features do not match the criteria for massive mechanized construction [18]. (4) Post-inspection is not time-sensitive. The results of the quality assessment cannot be directly relayed to the construction staff on-site during the compaction process, because the compaction quality outcomes are often judged after the construction is finished. This leads to unavoidable over-compaction or under-compaction during the construction process, which can easily result in project delays due to the need for rework [11].

Researchers have suggested using digital compaction technologies to address the issues existing in conventional compaction techniques. The digital compaction method is to develop a digital construction management system by installing a positioning system on the roller, enabling real-time observation of the number of rolling passes and the roller's trajectories, eliminating the drawbacks of manual supervision and management [19, 20]. The digital compaction method has further developed into a continuous compaction control method with the advent of continuous compaction indicators, which entails mounting sensors on rollers to achieve compaction quality control through continuous detection of

compaction quality and real-time monitoring of compaction parameters [21–23]. Compared with the number of rolling passes method, the continuous compaction control method can control the compaction process, that is achieving real-time control of the overall compaction quality and uniformity of the compaction surface. However, there are still many challenges that warrant further consideration. For instance, the evaluation of compaction quality still depends on human judgment, and the application of manual driving always results in control errors.

To solve the above-mentioned problems, some researchers have proposed an automatic rolling method based on unmanned technology [24–27]. The automatic rolling method allows the roller to operate according to pre-set instructions by modifying the roller, which mitigates the impact of human error and enables precise control of the roller. However, feedback control of the filling's compaction quality still relies on human decisions, i.e., the compaction quality needs to be judged offline before the next step can be taken. With the development of sensor technology, automatic control technology, and artificial intelligence, the intelligent compaction method has become a new solution to achieve autonomous sensing, autonomous decision-making, and autonomous control by incorporating intelligent algorithms in the decision-making function [4, 16, 28–30]. The intelligent compaction method avoids unnecessary waste in the construction process and truly achieves energy-saving, environmentally friendly, green and efficient intelligent construction.

At present, the existing intelligent compaction methods are mainly for vibratory compaction, while our research on intelligent compaction of airport high fill is for impact compaction. Therefore, the research on three key issues of impact compaction in intelligent compaction is summarized, including compaction quality evaluation

algorithm, dynamic optimized path planning and implementation of unmanned technology.

Indeed, advancements and achievements in intelligent compaction methods play a pivotal role in enhancing the management of compaction quality in earthwork. The research has shown that these potential directions include coupling problems of multiple indicators in intelligent evaluation algorithms, unmanned roller groups collaborative control problems, and intelligent decision-making and optimization problems of multi-vehicle compaction paths. To provide a comprehensive overview of the current compaction quality control methods, and to identify potential challenges and outline future research directions in this field, this paper reviews the literature on the methods of compaction, systematically narrates the current development of compaction quality control methods in the field of geotechnical engineering, and summarizes the work that has been done. The various compaction quality control methods and their corresponding issues are summarized in Sects. 2 to 5, and the main topics in contemporary intelligent compaction are discussed in Sect. 6, and the current research work and a vision for the future are summarized in Sect. 7.

## 2 Traditional compaction method

### 2.1 Compaction technology control method

The rolling passes control method and traces control method for rolling wheels are widely employed empirical compaction technology control methods at the moment.

#### 2.1.1 Rolling passes control method

The control criteria for the number of rolling passes are determined by ensuring that the compaction achieved in the rolling test meets the required standards. However, strict requirements must be met when utilizing rolling passes to control the compaction quality. These include ensuring that the filling type, filling height, and underlying soil layer of the rolling section match those of the test section. Moreover, the roller's rolling parameters must be entirely consistent [31], as shown in Fig. 2.

However, the compaction passes control method is an outdated manual management approach, which is

susceptible to human error and is prone to misjudgment of compaction passes. The poor precision of the compaction quality control in this method will result in under-compaction, miss-compaction, and over-compaction in the whole construction area.

#### 2.1.2 Traces control method for rolling wheels

The traces control method for rolling wheels uses "no wheel trace" as the indicator of the completion of compaction, essentially controlling the degree of plastic deformation of the filler. However, this approach faces two significant issues. Firstly, whether the compaction state achieved "no wheel marks" is solely decided by the on-site construction staff making the decision relatively subjective. Moreover, this method is unable to evaluate the compaction quality quantitatively. Secondly, even if the plastic deformation of coarse-grained materials has stopped, the structure's mechanical properties may continue to change, leading to potential inaccuracies in quality assessment using the rolling wheel traces control method [31].

### 2.2 Sampling point detection control method

To ensure that no issue would occur during the construction process, on-site supervision is typically provided. The compaction quality of the earthwork is then verified at predetermined sampling points when construction is complete. The compaction indexes of traditional evaluation for fill materials of earthworks are generally density, strength, modulus, etc.

#### 2.2.1 Physical indicator—density

There are two main reasons for using density as a compaction index. Firstly, the operation of the density test is simpler than the mechanical test; secondly, there is an underlying principle that the denser the filler, the stronger the resistance to deformation [31]. Indicators such as void ratio and relative density are utilized for non-cohesive soils, while the degree of compaction index is used for cohesive soils. The current methods for detecting density include the sand-cone method [32], cutting ring method [33], electromagnetic soil density

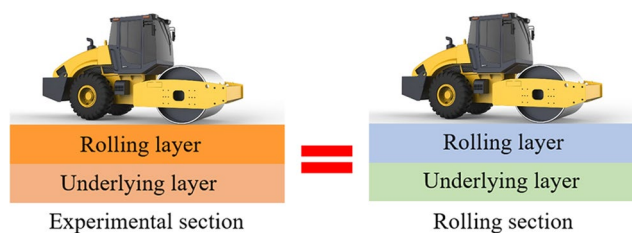


**Fig. 2** Application conditions of rolling passes control method (recreated based on the concept of [31])

gauge method [34], nuclear density gauge method [35], and non-nuclear density gauge method [36], etc. Figure 3 illustrates some of the testing equipment used.

**2.2.2 Mechanical indicators—strength and modulus**

The compacted filler body serves to support both the upper structural load and vehicle load, making it crucial to have adequate deformation resistance. Mechanical indicators can be categorized into strength and modulus indicators. California bearing ratio (CBR) and impact test value (CIV) are examples of strength indicators. The dynamic cone penetrometer (DCP) method [37] and the Clegg impact soil test (CIST) method [38] are two techniques frequently used to measure strength. Modulus indicators include deformation modulus  $E_{v2}$ , rebound modulus  $E$ , dynamic modulus  $E_{vd}$ , and foundation reaction coefficient  $K_{30}$ , etc. The lightweight deflectometer

gauge (LWD) method [39, 40], the soil stiffness gauge (SSG) method [41], and the plate load test (PLT) method [42] are some of the frequently employed techniques for determining modulus. Figure 4 displays some of the testing equipment used. The characteristics of the sampling point detection method are shown in Table 1.

But the following issues with the sampling point detection method still need to be resolved: (1) If the distribution of fillings is uneven, the results of the compaction quality distribution will not follow a normal distribution, so the sampling test results are not necessarily representative and cannot accurately reflect the compaction state of the whole construction area; (2) Some detection methods are destructive and time-consuming, which seriously hinders the progress of the construction; (3) The results of the compaction quality inspection cannot be recorded in real-time, so the record may be falsified; (4) During



**Fig. 3** Device for detecting density. **a** sand-cone cylinder. **b** cutting ring. **c** nuclear density gauge. **d** non-nuclear density gauge

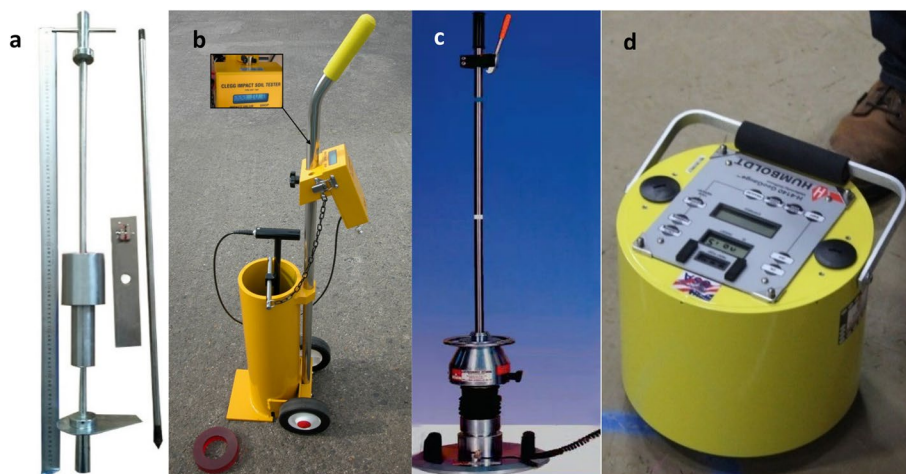


**Fig. 4** Equipment for testing mechanical indicators of soil. **a** DCP. **b** CIST. **c** LWD. **d** SSG

**Table 1** Characteristics of sampling point detection method

Sampling detection method	Indicators	Methodology evaluation
Sand-cone method	Dry density	Simple operation, but the improper operation is easy to cause large errors, and the test is time-consuming and damaging to the foundation
Cutting ring method	Dry density	Easy to operate, but it is not suitable for aggregate or loose material, and damaging to the surface
Electromagnetic soil density gauge method	Dry density	Non-destructive testing, convenient and time-saving, no need for standard block calibration, but need to set pre-parameters
Nuclear soil density gauge method	Dry density	The operation is simple and time-saving, but radioactivity requires the calibration of standard blocks and dedicated personnel to operate
Non-nuclear soil density gauge method	Dry density	Convenient, time-saving, non-radioactive, requiring standard block calibration, complex calibration, and poor testing accuracy
Dynamic cone penetrometer method	CBR	Fast, easy, no site restrictions, but time-consuming and time-sensitive
Clegg impact soil test method	CIV	Simple, easy to operate, time-consuming, and requires effective filtering of noisy signals
Light weight deflectometer gauge method	E	Low operating cost, however, has a poor correlation with compactness and high variability in measured values
Soil stiffness gauge method	E/CBR	Portable and user-friendly, fast measurement and high usability, but the test data are discrete in nature
Plate load test method	$E_{vd}$	No disturbance to the foundation soil, reliable results, but time-consuming and time-sensitive

the compaction process, the factors that need to be controlled include not only the degree of compaction but also the stability and uniformity of compaction. However, this requirement is not competent for traditional compaction sampling detection methods [31].

### 3 Digital rolling compaction method

To achieve process control for compaction, researchers have developed a digital construction management system that monitors compaction parameters and compaction conditions in real-time, known as the digital compaction method. The digital compaction method is divided into two categories based on different compaction quality control indicators: the rolling passes control method and the continuous compaction control method.

#### 3.1 Rolling passes control method

The number of rolling passes is used as the control indicator of compaction quality, and the digital construction management system developed by introducing the navigation and positioning system can achieve real-time, continuous and automated monitoring of the construction quality of the filling project by monitoring the number of compaction passes and the compaction trajectory [43].

The current methods for calculating the number of rolling passes include the grid calculation method [44–48], the pixel point method [49], and the image analysis method [50], respectively.

The real-time monitoring system for compaction quality is generally divided into three parts: (1) Monitoring center. The monitoring center is the core of the system,

mainly responsible for data processing, analysis, and other work of the system. Subsequently, all parties can communicate through the network and view construction quality information in real-time through the operating platform; (2) Database center. The database center is responsible for storing and managing all data in the system, ensuring the security and stability of data; (3) Navigation positioning and transmission terminal. Navigation and positioning are divided into reference stations and mobile stations. The reference station is fixed and installed in an open area near the construction area, while the mobile stations are installed on the road roller. These stations gather real-time positioning data and transmit it to the database center through network signals [45–49]. The common real-time monitoring scheme for compaction quality is shown in Fig. 5.

Strict requirements exist for controlling the number of rolling passes. It's necessary to compare several experimental sections before compaction, and the test conditions and rolling parameters of these sections should be consistent with the rolling section. However, ensuring these conditions during actual on-site construction can be challenging. Subsequently, the number of rolling passes needs to be constantly optimized due to the complexity of road bases or pavement materials used in construction sites. Therefore, the number of rolling passes is a macroscopic and empirical control method that cannot achieve fine control accuracy. To swiftly obtain information on the compaction quality of fillings, researchers have proposed continuous compaction indicators, and the continuous compaction method was born.

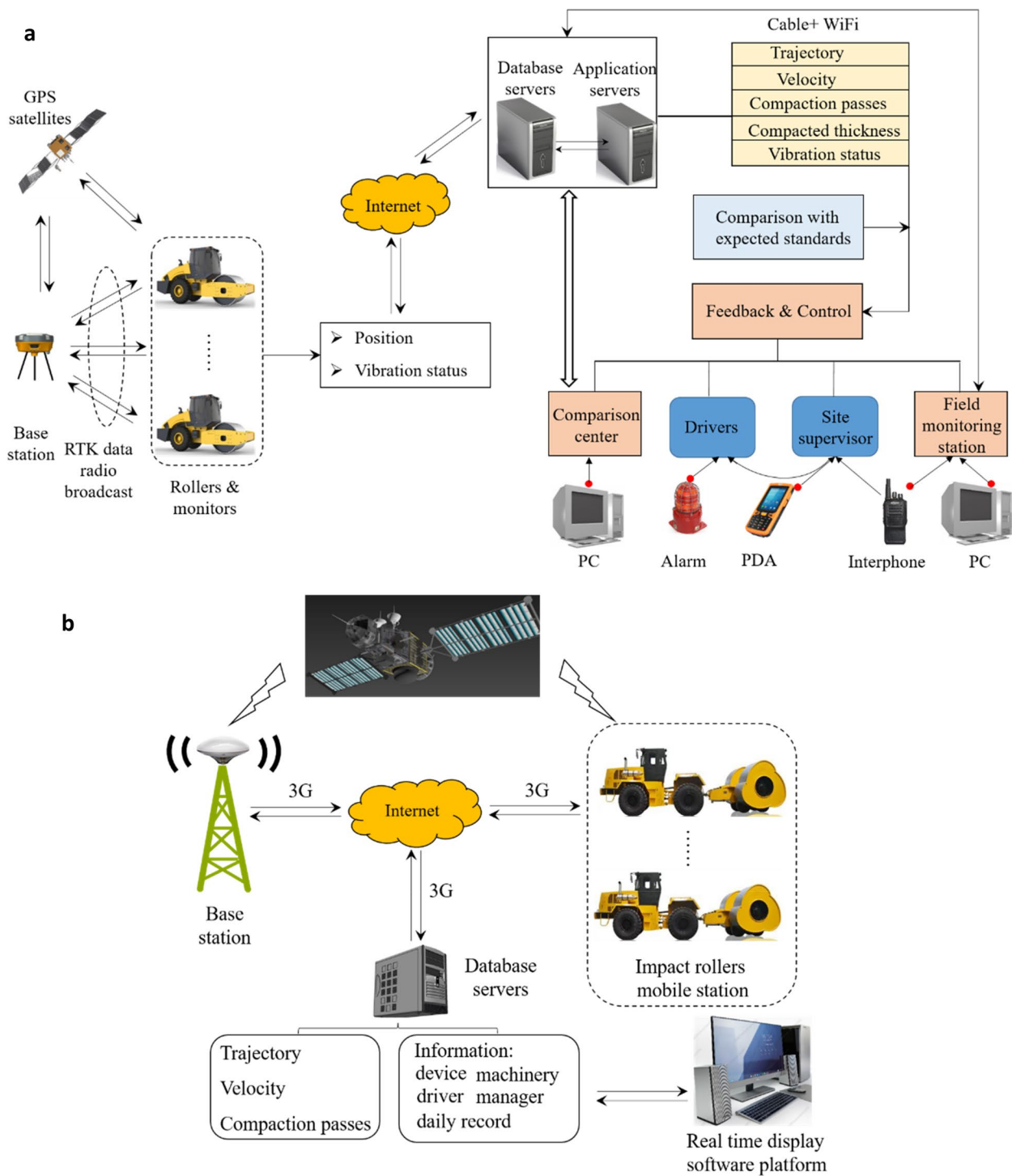


**Fig. 5** Digital compaction quality monitoring system. **a** Schematic diagram of real-time compaction quality monitoring for the core rock-fill dam (recreated based on the concept of [45, 46]). **b** Real-time monitoring scheme for impact compaction of airport high embankment (recreated based on the concept of [47])

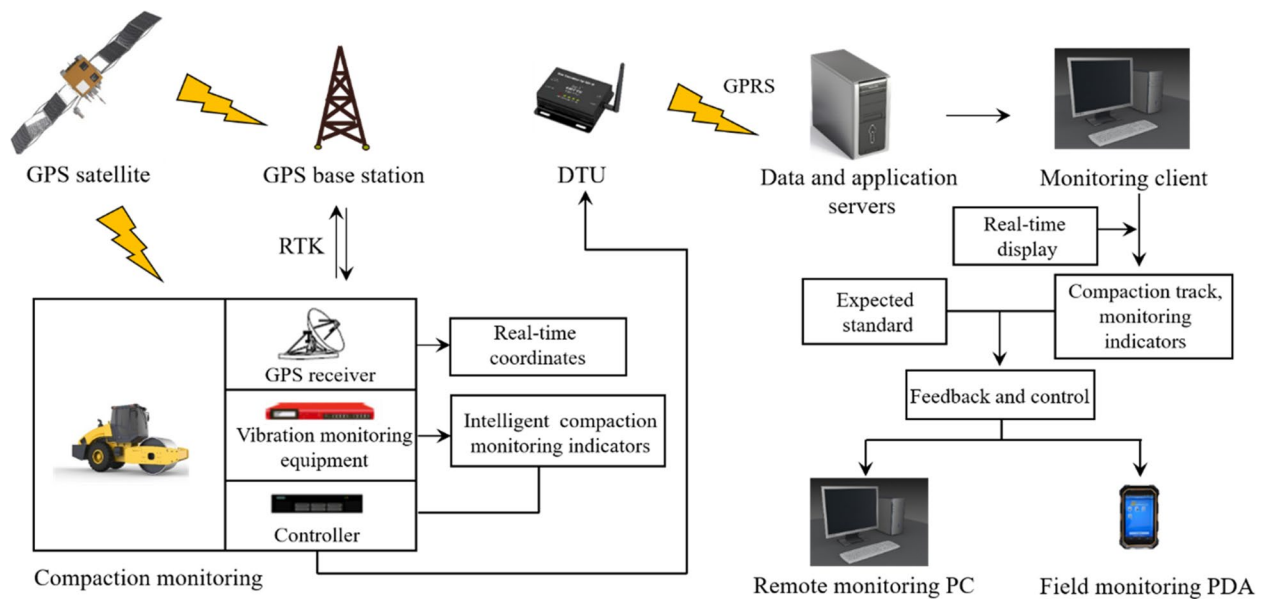


**Fig. 6** Continuous compaction control quality monitoring system (recreated based on the concept of [54] (AICV))

### 3.2 Continuous compaction control method

In 1975, the compaction meter co-developed by GEO-DYNAMIK and DYNAPAC in Sweden was applied to vibratory rollers, achieving the initial version of continuous compaction monitoring and control [51]. Then, the concept of continuous compaction control was formally presented in the early 1990s [52].

The continuous compaction control method involves evaluating the compaction conditions by monitoring the vertical vibration response signal for the vibrating wheel of the roller during the compaction process, and then the relevant compaction parameters and compaction conditions are visualized to guide the field compaction, which ultimately results in real-time monitoring and feedback control for the compaction quality of the whole construction area [53]. Figure 6 depicts the current continuous compaction monitoring system.

Continuous compaction control research primarily focuses on two aspects: the investigation of continuous monitoring indicators and the development of compaction quality evaluation methods. The following section describes the existing continuous monitoring indicators and compaction quality evaluation methods.

#### 3.2.1 Continuous monitoring indicators

At present, researchers have proposed a series of indicators for continuous monitoring of compaction quality, such as acceleration indicators, seismic wave velocity indicators, indicators based on roller-soil interaction, acoustic compaction amplitude indicators, and other indicators, which have been applied in scenarios like

roads [1–3], airports [5, 6], dams [9–11, 56], and railroads [13], and so on.

Acceleration indicators can be classified into two categories: acceleration frequency domain indicators and acceleration time domain indicators. The earliest proposed acceleration frequency domain indicator was the compaction meter value (CMV) [57], which used the ratio of the second harmonic amplitude of vibration acceleration to the fundamental frequency amplitude. Subsequently, other frequency domain indicators had also been proposed, such as compaction value (CV) [11], compaction control value (CCV) [58], acceleration intelligent compaction value (AICV) [54], total harmonic distortion (THD) [59–61], resonant meter value (RMV) [62], oscillometer value (OMV) [63], turbulence factor ( $F_t$ ) [64], etc. The time-domain indicators of acceleration include peak acceleration ( $a_p$ ) [56, 65–67], root mean square acceleration ( $a_{rms}$ ) [56, 67], and peak acceleration factor (CF) [56, 68].

In addition to acceleration indicators, researchers have employed the seismic wave approach to assess the compaction quality of rockfill. Seismic wave indicators can be classified into three categories based on propagation mode: longitudinal wave velocity (P-wave) [69], transverse wave velocity (S-wave) [70, 71], and surface wave velocity (L-wave) [72]. Furthermore, indicators derived from roller-soil interaction have been utilized, such as machine drive powder (MDP) [73], dynamic elastic modulus ( $E_{vib}$ ) [74], material stiffness ( $K_s$ ) [75], structural resistance (VCV) [76], and foundation reaction force ( $F_s$ ) [77]. In addition, researchers have also proposed other

**Table 2** Classification of continuous monitoring indicators

Type	Indicators	Interpretation	Formulation
Acceleration frequency domain indicators	CMV	the ratio of second harmonic amplitude to fundamental frequency amplitude	$CMV = C_1 \frac{A_{2\Omega}}{A_{1\Omega}}$ [57]
	CV	the ratio of second harmonic amplitude to fundamental frequency amplitude	$CV = C_2 \frac{A_{2\Omega}}{A_{1\Omega}}$ [11]
	CCV	the use of more harmonic frequency components to determine	$CCV = C \frac{A_{0.5\Omega} + A_{1.5\Omega} + A_{2\Omega} + A_{2.5\Omega} + A_{3\Omega}}{A_{0.5\Omega} + A_{1\Omega}}$ [58]
	AICV	multi-harmonic frequency component calculation formula	$AICV = C \frac{A_{1.5\Omega} + A_{2\Omega} + A_{2.5\Omega}}{A_{0.5\Omega} + A_{1\Omega}}$ [54]
	THE	considering the higher harmonic components	$THD = C \frac{\sqrt{A_{2\Omega}^2 + A_{3\Omega}^2 + \dots + A_{n\Omega}^2}}{A_{1\Omega}}$ [61]
	RMV	the ratio of half harmonic amplitude to fundamental amplitude	$RMV = C \frac{A_{0.5\Omega}}{A_{1\Omega}}$ [62]
	OMV	the product of the first-order derivative of horizontal acceleration and period	$OMV = \left  \frac{d}{dt} \left( \frac{\partial^2 x}{\partial t^2} \right) t_{per} \right $ [63]
	$F_t$	vibration factor	$F_t = \frac{\sum_{i=1}^3 S_i + \sum_{i=1}^3 S'_i}{\frac{S_0 + S'_0}{F_j (m_1 + m_2) g}}$ [64]
Acceleration time domain indicators	$a_p$	peak acceleration	$a_p = \max \{  a_i  \} (i = 1, 2, \dots, n)$ [56]
	$a_{rms}$	root mean square acceleration	$a_{rms} = \sqrt{\frac{a_1^2 + a_2^2 + \dots + a_n^2}{n}}$ [56]
	CF	peak acceleration factor	$CF = \frac{a_p}{a_{rms}}$ [56]
	Indicators based on roller-soil interaction	MDP	mechanical drive power for static rollers
$E_{vib}$		dynamic modulus of elasticity, which is only a quasi-dynamic modulus	$Z_d = \frac{2(1-\eta^2)F_s}{\pi LE_{vib}} \left( 1.886 + \ln \frac{t}{\beta} \right)$ [74]
$K_s$		material stiffness, which is a hypothetical index	$K_s = 4\pi^2 f^2 \left( \frac{m_d + m_{efe} c p s \phi}{a} \right)$ [75]
VCV		structural resistance	$VCV = P \sin \omega t + Mg - \eta Mf(\ddot{u}, \omega)$ [76]
$F_s$		foundation reaction force	$F_s = m_e f_e \omega^2 - m_d a_m$ [77]
$F'_s$		Improved foundation reaction force	$F'_s = m_e f_e \omega^2 - m_d a_m \cos(180^\circ - \Delta\varphi)$ [77]
ECP		effective compaction power	$ECP = P_g - 2\pi^2 f^2 (c_1 A_x^2 + c_3 A_y^2) - VG[\sin \varphi + (1 - \zeta) \frac{a}{g}] - (mV + b)$ [67]
Seismic wave indicators	$V_p$	longitudinal wave velocity	$V_p = \sqrt{\frac{E}{\rho} \frac{1-\nu}{(1+\nu)(1-2\nu)}}$ [69]
	$V_s$	transverse wave velocity	$V_s = \sqrt{\frac{G}{\rho}}$ [70]
Ground-penetrating radar indicator	$\epsilon_{ac}$	dielectric constant	$\sqrt{\epsilon_{ac}} = \theta_s \sqrt{\epsilon_s} + \theta_{aw} \sqrt{\epsilon_{aw}} + \theta_{air} \sqrt{\epsilon_{air}}$ [78]
Acoustic compaction value	SCV	the product of the calibration coefficient of the compacted materials and the second harmonic component of the effective acoustic wave spectrum	$SCV = k \times A_2$ [10]
Energy indicators	Omega	The hysteresis circle area characterizes the energy absorbed by the soil during one vibration cycle	$W_{eff} = \oint_{2T} [-(m_D + m_E) \ddot{z}_1 + \bar{F}_{stat} + \bar{F}_E] \dot{z}_1 dt$ [79]
	CEV	Characterize the amount of energy carried by the nonlinear vibration signal	$e(\omega, t) = \int_{-\infty}^{\infty} Re \sum_{i=1}^{n+1} a_i(t) \cdot e^{j \int \omega_i(t) dt}$ [80]
	DMV	The energy dissipated per unit volume and per unit damping in unit time	$DMV = \pi \omega_0^3 \int_0^{+\infty} \frac{A^2}{\omega^3} d\omega$ [81]

indicators, such as acoustic compaction value (SCV) [10], ground-penetrating radar signal peak coefficient index [78], and energy indicators, such as Omega [79] \cdot CEV [80] \cdot DMV [81], etc. The specific details of above mentioned indicators are shown in Table 2.

**3.2.2 Evaluation methods for compaction quality**

The compaction quality is influenced by a wide range of variables, including material parameters and compaction parameters. Numerous methods currently exist for establishing compaction quality models,



**Table 3** Multi-indicators compaction quality evaluation methods

Methods	Parameters	Reference
Linear regression model	SCV, P5	[10]
	CMV, E	[18]
	ECP, NMAS	[67]
	$f$ , CV	[77]
	E, THD	[82]
	CMV/VCV, $\nu$ , $a_p$ , $f$ , $\nu$ , $\omega$	[93]
	CV, $\omega$	[95]
Multiple-nonlinear regression model	$n, h, \nu, J, \omega, p$	[9]
	SCV, P5	[10]
	CV, $\omega$	[11]
	ECP, NMAS	[67]
	E, THD	[82]
Customized kernel support vector regression model	N1, N2, N3, $V, h, W, P5, C_{ur}, C_c, A_f, A_{h1}$	[89]
Support vector regression model	P5, MPS, AMMC, HVP, SRP, RT, RV	[90]
GA-SVM model	$V, \omega, G, M$	[91]
Artificial neural network model	$\nu, J, n, h$	[84]
	$N, H, N^*, \omega, C_{ur}, C_c$	[85]
	$h, \omega, \nu, p$	[86]
	CMV, $\nu, f, d$	[87]
	$M_{sw}, M_{sp}, M_{RD}, C_{MM}, C_{MT}$	[96]
	$C_{RT}, C_{RV}, C_{RD}, C_{RP}, M_{MT}, M_{MH}$	

including regression models [10, 11, 82, 83], neural network models [84–87], support vector machine models [88–91], fuzzy control models [86, 92], etc. Regression models can be further subdivided into linear regression models [2, 10, 11, 93, 94] and nonlinear regression models [56, 66, 67].

Currently, single-index compaction quality evaluation predominantly utilizes linear and non-linear regression methods. Zhu et al. [2] established a linear regression model between CMV and dry density of the sub-base, indicating a strong linear correlation. Zhang et al. [10] established a linear regression model between SCV and dry density of rockfill, which showed a strong linear correlation between them. Liu et al. [11] established a linear regression model between CV and compaction degree (dry density) of gravel mixed cohesive soil and rockfill material, and the results showed a strong linear relationship between CV indicator and compaction degree. Xu et al. [66] established a nonlinear regression model between the  $a_p$  index of loess filling and the compaction degree of each layer of soil, with correlation coefficients greater than 0.92. Hua et al. [56] established linear regression models and hyperbolic regression models for  $a_p$ , CMV, CF, and void ratio (relative dry density) of primary and secondary rockfill, respectively.

Given the low accuracy of models that rely solely on vibration signals without considering the properties of

compaction materials, researchers have proposed multi-indicator compaction quality evaluation methods. These methods integrate the properties of compaction material parameters and vibration signals, as demonstrated in Table 3.

#### 4 Automated compaction method

With the advancement of unmanned driving technology, researchers have proposed an automatic compaction method to address the challenges caused by manual driving. This method is developed based on the continuous compaction control approach, which modifies the roller’s control system to enable unmanned operation. The travel, reversing, and steering systems of the roller are all designed as automated elements that can be controlled using commands.

The first automatic control roller was used in asphalt pavement construction in Japan in the 1980s [97]. Following the swift progress of driverless technology in China, various universities sequentially developed unmanned vibratory roller systems, including Tsinghua University [98–100], Tianjin University [101, 102], Beihang University [103], Shanghai Jiao Tong University [104], Southeast University [105], Tongji University [106], and Chang’an University [107], et al. China Institute of Water Resources and Hydropower Research [108], China Academy of Railway Sciences Limited

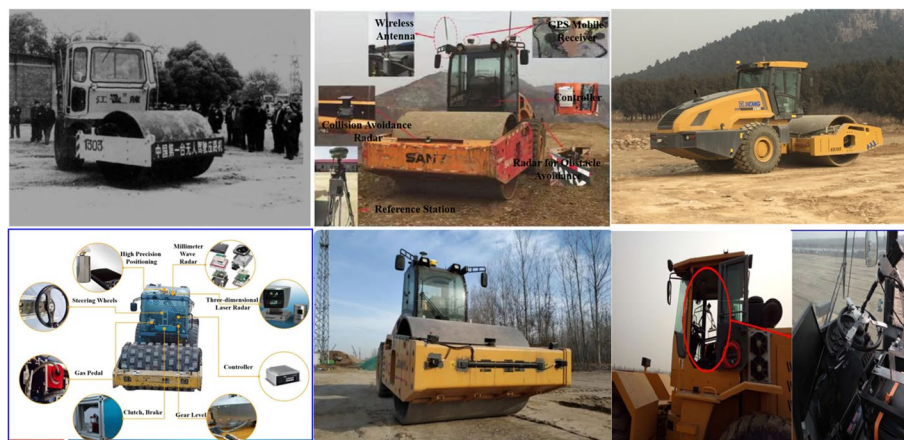


**Fig. 7** Unmanned rollers developed by various institutions [4, 7, 100, 108, 110]

[109], and other companies have also conducted relevant research and engineering applications. Unmanned road rollers are shown in Fig. 7.

The National University of Defense Technology developed China's first unattended roller, accomplishing basic functions like steering and parking [110]. Subsequent to these developments and evolving theories, a variety of unattended rollers were successively introduced. China Water Resources and Hydropower 5th Engineering Bureau and Tongji University jointly developed an unattended vibration roller modified by hydraulic steering [111]. Liu et al. [98, 99] from Tsinghua University developed a set of automatic driving systems of vibratory roller for hydraulic construction, in which the steering mechanism was modified by an electric steering wheel. Zhong et al. [101, 102] from Tianjin University has developed an unattended vibration roller system, which also achieves automatic steering control by modifying the steering mechanical structure. Yu et al. [103] from Beihang University developed an automatic steering control mechanical structure called a robotic arm, which is used to control the steering wheel, brake, throttle, and gears. Luo et al. [104] from Shanghai Jiao Tong University designed an unattended intelligent vibration roller and its system, using modified electric actuators. Huang et al. [112] designed an autonomous construction system for unattended vibration rollers with PLC as the core controller. Currently, research on automatic compaction methods primarily focuses on the following areas:

### 1. Positioning technology

Currently, both Beidou and GPS positioning systems are commonly installed on unattended vehicles, but they have inadequate anti-interference ability in complex

situations. To cope with this, researchers have studied additional positioning techniques to improve accuracy in complex environments. With the help of laser emission devices, Gao et al. [105] created an unattended roller system that successfully makes up for the drawbacks of conventional single positioning techniques. An unattended rolling system that uses LiDAR range to assist in positioning in challenging situations devoid of positioning signals was created by Tsinghua University and Sichuan Chuanjiao Road and Bridge Corporation [113].

### 2. Path tracking

The path-tracking accuracy of unattended rollers is directly related to the quality and efficiency of compaction, and the research on path-tracking control of unattended rollers in China mainly includes the team of Xie from Tianjin University, Bian from Tongji University, and Liu from Tsinghua University. Bian et al. [106] studied a path-tracking control method based on a fuzzy control algorithm, which improved the performance of automatic rolling. The unattended roller developed by Yao et al. [114] comes with anti-interference and heading estimation methods, which can achieve accurate trajectory tracking. Song et al. [115] proposed a path-tracking control framework for unattended rollers to suppress composite disturbances. Fang et al. [116] considered the impact of roller vibration and designed a path-tracking control model to achieve the automatic rolling of unattended rollers. Song et al. [7, 117] designed a path optimization method for headland turning to address the significant tracking errors that often experience at the turning point for unattended impact rollers, effectively improving the turning tracking accuracy.



**Fig. 8** On-site Construction scene for unmanned roller fleets [122–124]. **a** Panzhuhua-Dali Expressway. **b** Beijing-Xiongan Expressway. **c** Yangliu-Xuanwei Expressway. **d** The Viaduct in Shanghai

### 3. Obstacle identification

Identifying obstacles is crucial in the complex construction site environment where a roller may encounter moving or stationary obstructions. Chen et al. [108] created an unmanned roller system utilizing technologies such as LiDAR, shortwave radar, and satellite positioning, which are capable of performing tasks including obstacle recognition, path planning, path tracking, and obstacle avoidance. In order to identify filler and obstacles, Ye et al. [109] applied technologies like unmanned, continuous compaction detection, and image recognition to intelligent rollers. The obstacle avoidance functions of the autonomous rolling system created by Zhang et al. [100] have been effectively applied to the compaction quality control of rockfill materials for earth-rock dams.

### 4. Path planning

Path planning is an important research topic for unmanned rolling technology. Path planning is mainly divided into two types: static path planning and dynamic path planning. Zhang et al. [8] proposed an optimal dynamic path planning algorithm for the impact roller based on the rolling passes as the compaction quality

control index. The automatic driving control system of impact rollers developed by Zhang et al. [118] has added the function of static path planning, achieving the cyclic multiple rolling of compaction machinery. Shi et al. [119] established a time–cost function for unmanned roller group operations based on the chaotic dragonfly method. With the principle of minimizing time cost, the task of fully covering the working face path was assigned to the roller groups, achieving efficient and collaborative compaction operations among all rollers. Shi et al. [120] further studied the collaborative control problem of multiple unmanned rollers, as well as the optimal compaction path planning problem and optimal compaction parameter determination problem of multiple unmanned rollers.

### 5. Collaborative control of multiple unmanned rollers

In large-scale construction tasks, a single roller is often insufficient, necessitating the deployment of multiple unmanned rollers on the construction site for cooperative compaction operations. Tsinghua University, in collaboration with XCMG Group and Sichuan Road and Bridge Group, developed a cooperative construction system for unmanned vibratory roller groups. On May 27, 2020 [121]. On August 30 of the same year, the driverless

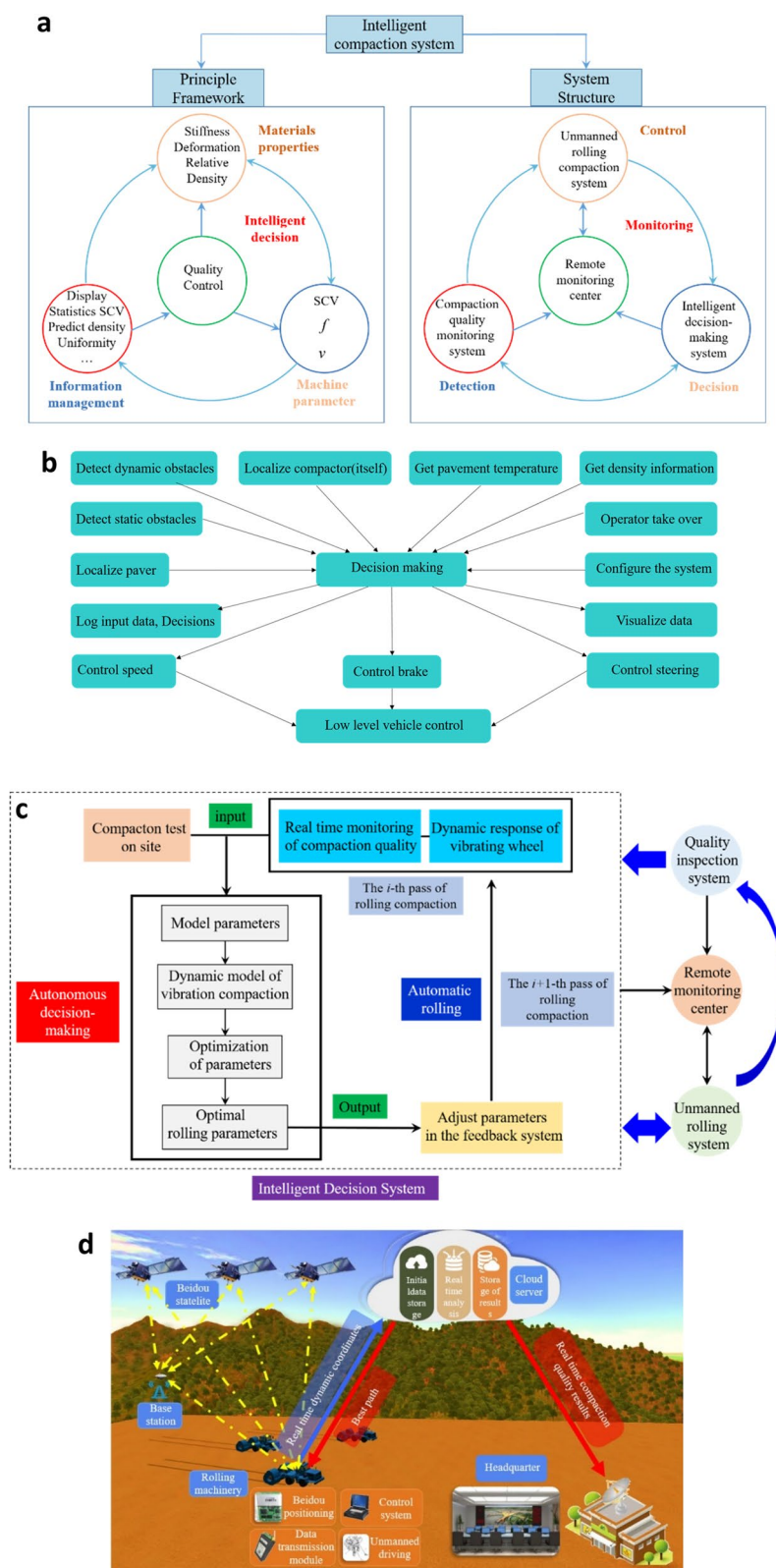


**Fig. 9** Intelligent compaction principle block diagram. **a** Framework and structure of the intelligent rolling compaction system (recreated based on the concept [16]). **b** Functional model for autonomous compactor (recreated based on the concept [125]). **c** Schematic diagram of intelligent rolling structure (recreated based on the concept [126]). **d** Schematic graph of intelligent compaction (recreated based on the concept [127])

construction machinery group developed by XCMG was applied for the first time in some sections of the Beijing-Xiongan Expressway, realizing the largest scale of unmanned cluster construction operation [122]. The unmanned roller fleet developed by Sany Heavy Industry Group has been used in numerous situations and locations around China in 2021, including the Yangxuan Expressway, Shanghai Dapo Viaduct, etc. [123], as shown in Fig. 8.

The automatic rolling approach still has several drawbacks, such as the inability to independently tune compaction parameters and the fact that compaction quality control is still accomplished by manual off-line decision evaluation.

## 5 Intelligent compaction method

The intelligent compaction method, which is appropriate for more complicated construction situations, is characterized by an autonomous decision-making function and automatic compaction without human intervention. Figure 9 depicts the current intelligent compaction system. Zhang et al. [16] designed an intelligent compaction system composed of four key elements: an acoustic monitoring system, an intelligent decision system, an unmanned compaction system, and a real-time remote monitoring center, respectively. Among them, the intelligent decision-making system integrates artificial intelligence algorithms and operations research to dynamically optimize the compaction parameters of the compaction process from a global perspective, as shown in Fig. 9a. Botev and Azidhak [124] developed an intelligent compaction system for asphalt pavement construction, including sensors and external systems, a vehicle system, an operating system, and a decision system, as shown in Fig. 9b. An intelligent compaction system for roadbed pavement developed by Lin and Wang [125] is composed of a quality inspection system, an intelligent decision system, an unmanned compaction system, and a remote monitoring center. The intelligent decision system is based on a machine learning or artificial intelligence neural network model to predict the compaction construction parameters of the new compaction area by analyzing the existing compaction quality information, and the intelligent decision system is shown in Fig. 9c. Yao et al. [4, 126] developed an intelligent compaction quality monitoring system for airport high embankments based on technologies such as unmanned driving, virtual reality, the Internet of Things, and cloud computing. The upper monitoring platform can evaluate the compaction quality according to the monitored acceleration indicators, and determine the optimal path for the local area based on the compaction conditions. Following this, relevant compaction instructions are conveyed to the unmanned roller at the lower level to facilitate automatic

compaction. Concurrently, the system utilizes virtual reality technology to synchronously display the on-site construction situation. The construction principle is shown in Fig. 9d.

The intelligent compaction methods mentioned above are based on optimal paths, unmanned driving, intelligent decision making and other technologies that avoid unnecessary waste in the construction process and achieve a truly energy-saving, environmentally friendly, green and efficient intelligent construction, which is also consistent with the theme of sustainable cities [127].

## 6 Key technologies for intelligent compaction

There is no excitation force in the compaction parameters of impact rollers due to the difference between the mechanical structure of impact rollers and vibratory rollers. Consequently, decision-making does not necessitate the dynamic optimization of vibration frequency and amplitude parameters. For intelligent impact rollers, the compaction path is the focus of decision-making and must be dynamically optimized from a global perspective, considering both compaction efficiency and quality. As a result, the compaction quality evaluation algorithm, dynamic optimal path planning, and unmanned implementation are the three key technologies for intelligent compaction research.

### 6.1 Compaction quality evaluation algorithm

The key issue in intelligent compaction is to evaluate the compaction quality in real-time, specifically, to establish the relationship between acceleration and dry density. Physical property indices (i.e. dry density value  $\rho_d$  or compaction degree  $K$ ) are usually regarded as the compaction quality control indices for soil-filling, and the peak acceleration in continuous monitoring indicators is widely used. Therefore, the relationship between peak acceleration and dry density has been mainly studied. The current general method is to directly establish the relationship between peak acceleration and dry density, employing empirical formula based on limited field data. This approach has the following problems: (1) the relationship between peak acceleration and dry density is not so simple, and the expression of its function is uncertain. The function derived directly from human analysis may not accurately represent the true relationship and might only be applicable within a specific range. In some special cases, it may lead to invalid prediction in some cases. (2) The methods of formula fitting and parameter fitting lack reasonable scientific explanations and cannot reasonably reflect the development laws and trends of dry density change curves with complex coupling characteristics.

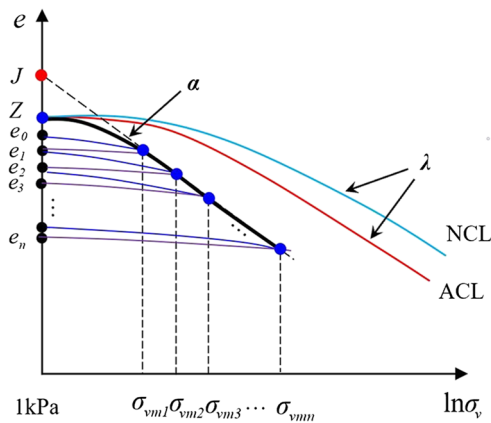


**Fig. 10** Sketch graph of compaction envelope for soil [127]

The relationship between peak acceleration and dry density is established from the perspective of the deformation mechanism. After detailed analysis, it reveals that the response of peak acceleration to dry density includes two different physical mechanisms. One is the response of peak acceleration to impact force, where the relationship between the force and the acceleration is by the kinematic law of objects. The other is the response of the void ratio of soil to the force, where the relationship between the force and void ratio of soil is by the constitutive law of soils. Firstly, the formula between peak acceleration and the impact was obtained based on the kinematic equation. Moreover, the deformation of soil is directly related to the stress on the soil. Therefore, the key to establishing the relationship between acceleration and dry density is to make clear the relationship between dry density (i.e. void ratio) and impact stress.

**6.1.1 Relationship between impact stress and impact acceleration**

Under the action of traction, the impact roller continuously keeps rolling forward until the wheels climb to the highest position, and then beats the ground and repeats, making the soil gradually become dense. For simplification of the analysis, the situation is modelled as a rammer impacting the soil, consisting of two stages, and excluding the rebound of the tamper after impact.

The first step is the free-falling process of the tamper where the tamper falls from the height *h* to the soil surface. The second step is the compaction process, where the tamper contacts the soil surface and moves downward with the soil until the speed decreases to 0.

When the displacement of the soil reaches the maximum, the peak value of impact stress on soil mass is expressed as

$$\sigma_{vm} = \frac{m(g + a_m)}{A} \tag{1}$$

where *A* is the bottom area of the rammer and *a<sub>m</sub>* is the peak acceleration.

**6.1.2 Relationship between impact stress and void ratio**

The relationship between impact force and the void ratio is established through theoretical analysis. The rammer compacts the soil surface 'N' times until the post-impact dry density of the soil meets the predefined requirement, at which point the impact is ceased. The distribution of compaction points consisting of the peak impact stress and the corresponding void ratio is shown in Fig. 10. The curve connecting all the compaction points is termed the 'compaction envelope', where the solid black line represents the compaction envelope, the solid red line represents the *K*<sub>0</sub> compression line (ACL), the solid cyan line represents the isotropic compression line of normally consolidated soil (NCL), and *λ* is the slope of the NCL and ACL in the *e*-ln(*σ<sub>v</sub>* + *p<sub>s</sub>*) plane. When *σ<sub>v</sub>* → ∞, ln(*σ<sub>v</sub>* + *p<sub>s</sub>*) is approximately equal to ln*σ<sub>v</sub>*. The solid blue line represents the compression curve for each impact, and the solid purple line represents the unloading curve, and the dashed black line represents the asymptote of the compaction envelope.

It is found that the shape and variation pattern of the compaction envelope drawn in Fig. 10 is similar to the form of the isotropic compression line of the soil defined in the UH model [126], and therefore the equation of the compaction envelope is defined as follows

$$e = Z - \alpha \ln \left( \frac{\sigma_{vm} + C}{1 + C} \right) \tag{2}$$

where *Z* is the void ratio at 1 kPa for the compaction envelope, and the starting point of the compaction envelope is unique for the same kind of soil.

With the increase of impact times, the compaction envelope eventually tends to a straight line, which is defined as the asymptotic line of the compaction envelope, as shown in Fig. 10. The asymptotic line equation is defined as

$$e = J - \alpha \ln \sigma_{vm} \tag{3}$$

where *J* is the intercept of the asymptotic line, and *α* is the slope of the asymptotic line.

It is necessary to explain the difference between the compaction envelope, the compression curve for each impact, and the *K*<sub>0</sub> compression curve. The compaction envelope is a special state curve, which describes the state of compactness of soil at each impact with a

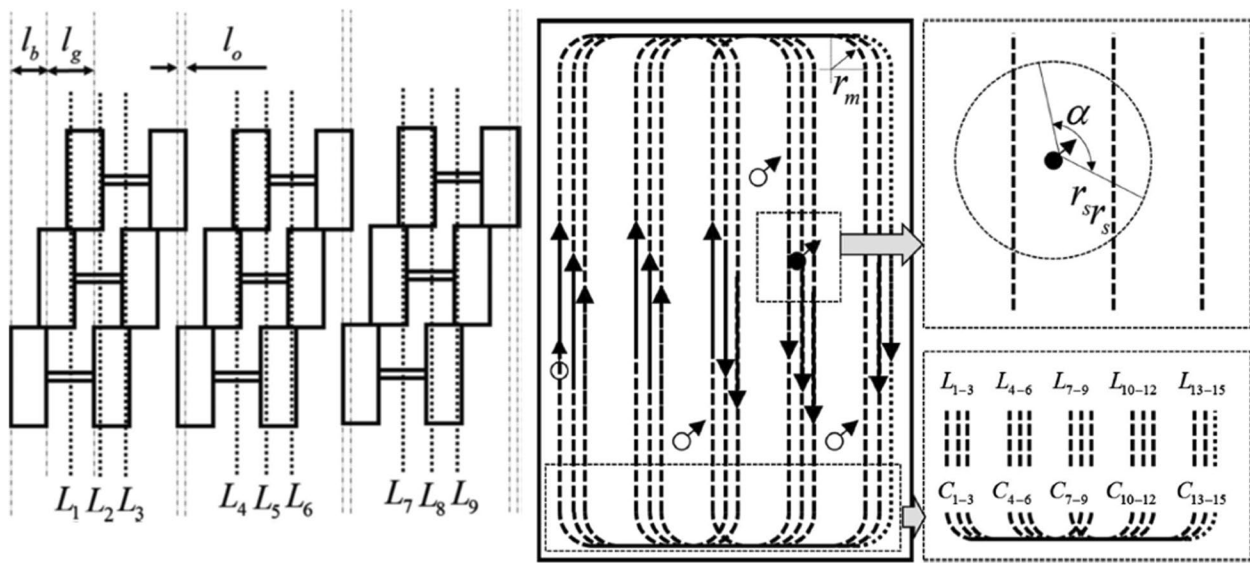


**Fig. 11** Design of the linear path [4]

certain impact parameter. The compression curve for each impact is a process curve, which describes the process of soil hardening at each impact. When the peak value of impact stress is large enough, the compression line converges to the  $K_0$  compression curve.

**6.1.3 Real-time calculation formulation for dry density**

Combining the corresponding relationship between void ratio and dry density, the real-time calculation formulation for dry density was acquired by coupling the above two equations [126].

$$\rho_d = \frac{G_s \rho_w}{J' - \alpha \ln \left( \frac{a_m + g}{B} \right)} \tag{4}$$

where  $J$  and  $\alpha$  represent the soil parameters,  $\rho_d$ , and  $a_m$  are the dependent variable and the independent variable respectively.

**6.2 Optimal path planning algorithm**

Currently, the driving path of impact rollers in construction is determined subjectively by machine operators. This will inevitably lead to over-compaction or under-compaction in some parts of the construction area, making uneven compaction of the filling soil and possibly triggering uneven settlement of the construction site in the future. It is necessary to reasonably design the optimal rolling path of the rolling machinery to ensure that the compaction uniformity and compaction quality of the entire site meet the requirements.

**6.2.1 Path design**

*Overlapping compaction method* According to the specifications requirements of compaction construction, the adjacent compaction range of wheels should have an overlap width of  $l_o$ . The schematic of the linear path design is shown in Fig. 11. The trajectory of the construction machinery is designed according to the setting of the size of the wheel and the overlap, such as lines  $L_1$ – $L_9$ . The first compaction in the far left area is completed after the impact compactor goes along the routes from  $L_1$  to  $L_3$ .

Considering the turning of machinery, it is required to connect linear paths with circular arcs, as shown in Fig. 11, and the number of linear paths in the quadrilateral surface may be even or odd. In the first case, the machinery should go through  $L_1$  and turn to  $L_8$ , which is in the middle of the surface. Along the direction marked in Fig. 11,  $L_2, L_9, L_3, L_{10}, L_4, L_{11}, L_5, L_{12}, L_6, L_{13}, L_7,$  and  $L_{14}$  are passed successively. However, in the second case, the machinery turns back to  $L_1$  and goes through the extra path  $L_{15}$  after it passes through  $L_{14}$ . No matter which case it is, the machinery can get back to the point where it starts. Then, during the compaction of the working surface, the machine uses the design radius  $r_s$  and the finite angle  $\alpha$  to delimit the search target location [4], as shown in Fig. 11.

*Non-overlapping compaction method* The manner of the overlapping generates unequal compaction areas in the horizontal direction, which leads to uneven compaction throughout the site and affects the compaction

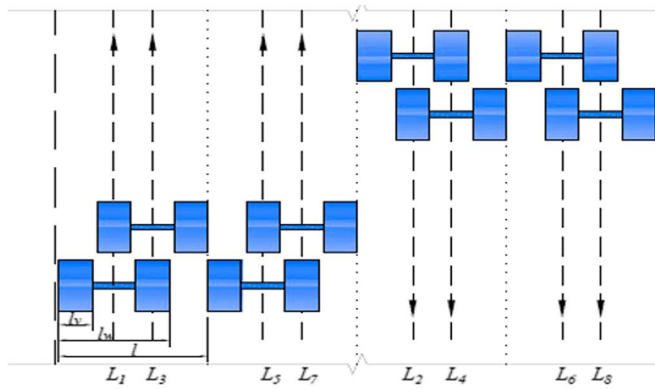


**Fig. 12** Path generation [8]

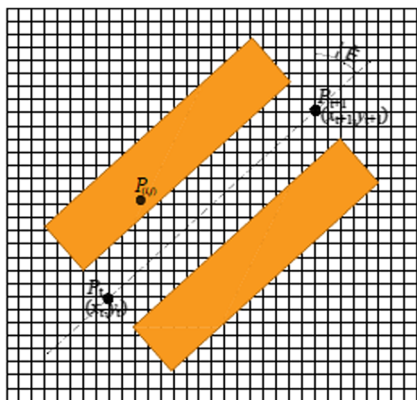
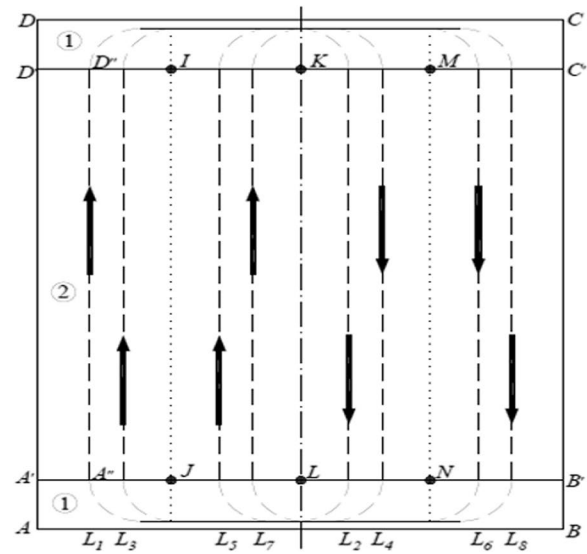


**Fig. 13** Calculate the acceleration value of the grid [8]

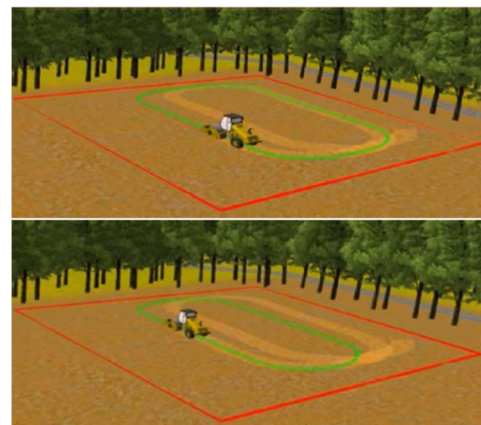


**Fig. 14** Schematic diagram of the optimal path [8]

quality. Therefore, the method of non-overlapping was proposed for compaction, as shown in Fig. 12. For the non-overlapping method of compaction, it is observed that there's a gap between two wheels from the parameters of the YP25. It is noted by the regulation that the non-overlapping method is reasonable and scientific as well as economically efficient.

According to the turning radius and width of the construction machinery, the working surface  $ABCD$  is divided into two parts: turning areas ① and working areas ②, where the coordinates of points  $I, J, K, L, M, N$ , and numbers of the rolling band can be calculated by the coordinates of points  $A', B', C', D'$ . Then the width of the rolling strip is calculated based on the construction technology of moving a wheelbase aside for impact rollers, and along the direction marked in Fig. 12,  $L_1, L_2, L_3, L_4$ ,

$L_5, L_6, L_7$ , and  $L_8$  are passed successively, and the path covering the entire working surface was generated [8].

### 6.2.2 Optimal path planning

*Calculate the acceleration value of grids* The trajectory of the impact roller is approximately straight between the time  $t$  and  $t+1$  because of the high frequency of Beidou, as shown in Fig. 13. Firstly, the heading angle of the impact roller, and the coordinates of the points  $P_t$  and  $P_{t+1}$  were obtained from the BeiDou positioning. Secondly, the acceleration data was bound by Beidou's positioning data to obtain the acceleration vibration signal at the corresponding position. Then, the characteristic value



of the signal, that is, the peak acceleration was extracted. Finally, the peak acceleration value was assigned to the attribute value at the grid P (*i, j*) under the wheel of the impact roller.

It is known that the grids covered by the impact roller are fixed when the machine works along the straight route of the full coverage path. Let *N* define the number of grids, and *a<sub>pi</sub>* is the attribute value of the *i*th grid. The average peak acceleration is given by the expression:

$$\bar{a}_p = \frac{\sum_{i=1}^N a_{pi}}{N} \tag{5}$$

*The planning of the optimal path* According to Eq. (5), the average acceleration peak of each strip in the construction area can be calculated respectively, and then the optimal path planning can be carried out, and the idea of the planning algorithm is as follows:

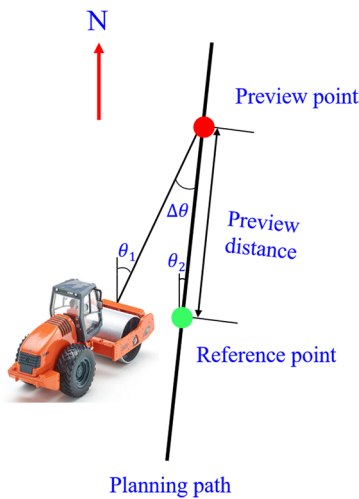


Fig. 15 Schematic diagram of lateral tracking control for the roller [7]

(1) When the impact roller passed the midline of the working surface(i.e., the line connecting the midpoint of *AD* and the midpoint of *BC*), the line segment *L<sub>left</sub>* or *L<sub>right</sub>* remains the same.

(2) The average peak acceleration of each strip on both sides of the rolling strip was compared in turn to get the minimum  $\bar{a}_p$  and the corresponding path number.

(3) The closed path was generated using the non-overlapping compaction method, the optimal path is shown in Fig. 14.

(4) The above steps were repeated until the compaction quality meets the requirements of the working face.

**6.3 Unmanned control for impact rollers**

The optimal path offers a straightforward method to correct the compaction trajectory for machine operators. However, the compaction effect is still heavily dependent on the behavior of machine operators, who often do not strictly follow the designated path. Thus, unmanned control technology is first applied to the implementation of the optimal path. The path-tracking control of rolling machinery is divided into two parts: longitudinal motion control and lateral motion control, both of which adopt the PID control method.

(1) The longitudinal control for the roller is the roller’s speed control. The roller is generally driven at a constant speed set before the vehicle starts during normal operation, and the current vehicle speed is obtained based on the speed sensor installed at the wheels. Then, the speed control amount determined by the difference between the current speed and the set desired speed is converted into a corresponding control command to the speed controller, and then the vehicle adjusts its gear to achieve acceleration or deceleration in one cycle.

(2) The lateral control for the roller is controlling the lateral distance, which is the distance between the actual trajectory of the roller and the desired path. Firstly, the

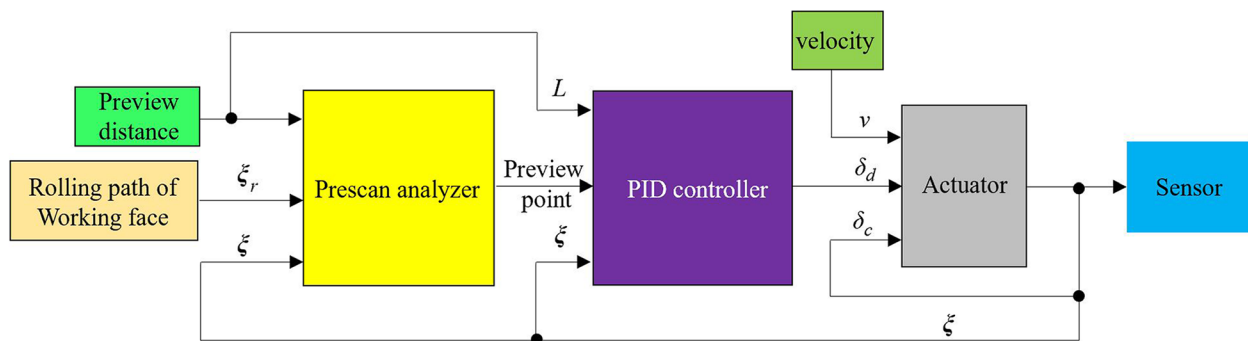
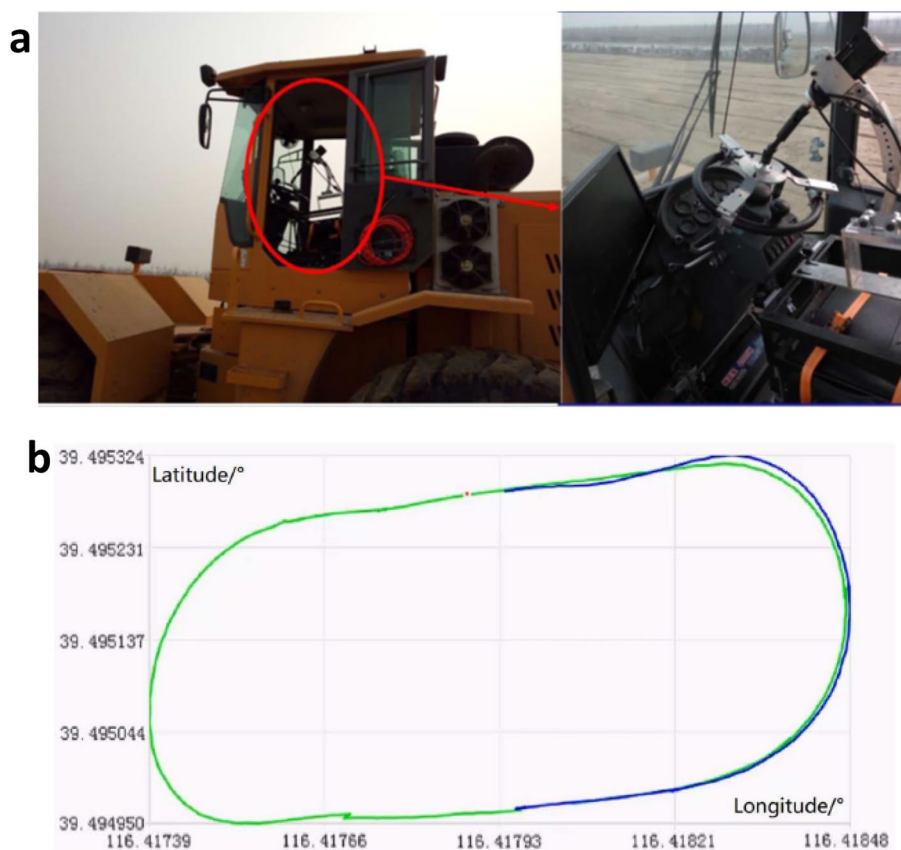


Fig. 16 Block diagram of lateral tracking control for the roller [7]



**Fig. 17** Unmanned driving system and tracking effect. **a** Unmanned driving control system [4]. **b** Actual trajectory tracking effect [128]

preview point on the planning path is determined based on the current position of the vehicle and the set preview distance. Then, the angle deviation  $\Delta\theta$  between the current heading angle of the roller and the target heading angle can be calculated from the position of the two points. Secondly, the desired steering angle of the roller is calculated by inputting the angular deviation into the upper PID controller. Thirdly, the angle deviation between the calculated desired steering angle and the actual angle detected by the sensor installed on the roller's wheel is calculated and inputted to the lower PID controller. Finally, the corresponding electrical signal is output to the servo motor to control the rotation of the steering wheel, achieving the desired turning angle. The schematic of lateral control is shown in Fig. 15.

The principle of the lateral tracking control system is shown in Fig. 16, where the reference rolling trajectory is  $\xi_r = (x_r, y_r, \varphi_r)$ , the actual trajectory of the roller is  $\xi = (x, y, \varphi)$ , and the desired control amount of steering wheel turning angle is  $\delta_d$ , while the actual turning angle of the actuator is  $\delta_c$ . The lateral tracking control system is divided into five parts: (1) Planning path module. The planning path module mainly receives instructions

from the upper controller, namely the rolling path of the working face; (2) Prescan analyzer. The prescan analyzer mainly provides appropriate preview points based on the set preview distance and current vehicle speed; (3) PID controller. The PID controller is mainly used to calculate the corresponding steering angle ( $\delta_d$ ) based on the current trajectory of the vehicle, the preview point, and the preview distance; (4) Actuator. The actuator achieves automatic steering control based on the current steering control command ( $\delta_d$ ) and the actual steering angle ( $\delta_c$ ); (5) Sensor module. The sensor module obtains the current front wheel angle ( $\delta_c$ ) and vehicle position of the vehicle ( $\xi$ ).

A robot has been designed to replace the driver, as shown in Fig. 17a. Firstly, the corresponding coordinate points on the planning path were found in the system database based on the real-time position of the impact roller during the operation, and the preview point was set at a certain distance in front of the machine. Secondly, the heading and steering angle of the impact roller was calculated based on the position of the preview point and the current point of the roller, and then the command was sent to the motor driver of the robot arm, which

would immediately execute the steering command. The actual effect of path tracking is shown in Fig. 17b.

By utilizing advanced technological means and intelligent methods, the proposed intelligent compaction method improves construction efficiency, reduces resource consumption, and decreases the negative impacts on the environment, thus contributing to the construction of sustainable cities.

## 7 Conclusion

(1) Based on their distinct characteristics, the existing compaction quality control methods are divided into traditional compaction methods, digital compaction methods, automated compaction methods, and intelligent compaction methods. It can be found that the digital compaction method achieves real-time monitoring of compaction quality and feedback control of the compaction process. The automated compaction method eliminates the influence of manual driving, and the intelligent compaction method integrates autonomous decision-making functions. All these methods solved some problems existed in traditional compaction methods respectively, but quite a few challenges and limitations need further investigation.

(2) The proposed intelligent compaction method for airport high fill mainly includes three key technologies. Firstly, the compaction envelope concept was proposed, and then the real-time calculation equation of dry density was established based on the equation of motion and the compaction envelope asymptotic equation, which can truly reflect the dry density variation law with complex coupling characteristics for compacted soil. Secondly, the developed dynamic optimal path planning algorithm takes into account both compaction efficiency and compaction quality, achieving intelligent compaction process optimization control. Thirdly, the designed robotic arm has been successfully equipped with the impact roller so that it has achieved the automatic driving function.

(3) Intelligent compaction methods are the trend of future development, but they present numerous challenges when dealing with complex environments, such as the coupling problem of multiple indicators in intelligent evaluation algorithms, unmanned roller groups collaborative control problems, and intelligent decision-making and optimization problems of multi-vehicle compaction path, etc.

### Acknowledgements

Thanks to Mr. Ran Wei for reviewing and correcting this manuscript.

### Authors' contributions

Yangping Yao: Conceptualization, Methodology, Formal analysis, Writing-original draft, Writing-review & editing, Supervision, Funding acquisition. Erbo Song: Investigation, Data curation, software, Writing-original draft, Validation. All authors have read and agreed to the published version of the manuscript.

### Funding

This paper was supported by National Natural Science Foundation of China (Grant No. 52238007, 51979001), and the National Key Research and Development Program of China (No. 2020YFB2103603).

### Availability of data and materials

Data sharing not applicable to this article as no datasets were generated or analysed during the current study.

### Declarations

#### Competing interest

The authors declare that they have no known competing financial interests or personal relationships that could have appeared to influence the work reported in this paper.

Received: 3 June 2023 Revised: 19 June 2023 Accepted: 21 June 2023  
Published online: 09 August 2023

### References

- Liu DH, Gong ST, Wei HY (2014) Fast assessment on compaction quality of highway subgrade based on real-time monitoring. *China Civil Eng J* 47(11):138–144. <https://doi.org/10.15951/j.tmgcxb.2014.11.049>
- Zhu XY, Bai SJ, Xue GP, Yang J, Cai YS, Hu W, Jia XY (2018) Assessment of compaction quality of multi-layer pavement structure based on intelligent compaction technology. *Constr Build Mater* 161:316–329. <https://doi.org/10.1016/j.conbuildmat.2017.11.139>
- Liu DH, Gao L, Lin M, Li ZL (2018) Real-time monitoring and assessment of compaction quality for highway asphalt pavements. *J Hohai Univ (Nat Sci)* 46(4):307–313. (in Chinese)
- Yao YP, Ruan YZ, Chen J, Geng Y, Zhang X, Liu BY, Zong XP, Yu GZ (2018) Research on a real-time monitoring platform for compaction of high embankments in airport engineering. *J Constr Eng Manag* 144(1):04017096. [https://doi.org/10.1061/\(ASCE\)CO.1943-7862.0001411](https://doi.org/10.1061/(ASCE)CO.1943-7862.0001411)
- Yao YP, Liu BY (2016) An evaluation algorithm of compaction quality for high embankment airports. *Ind Constr* 46(9):42–45. <https://doi.org/10.13204/j.gyjz201609010>
- Tang K, Yuan HW, Lv JX, Chen FC (2020) Research on the method for analyzing the degree of impact acceleration and compaction of the impact roller. *IEEE Access* 8:73588–73600. <https://doi.org/10.1109/ACCESS.2020.2983425>
- Song EB, Zhang X (2020) Research on the path optimization of unmanned rolling compaction for the high embankment of airport. *Jpn Geotech Soc Spec Publ* 8:142–148. <https://doi.org/10.3208/jgssp.v08.c05>
- Zhang X, Luo T, Song EB, Geng Y (2020) Algorithm for optimal path planning of impact roller in high-embankment airport. *Jpn Geotech Soc Spec Publ* 8:159–163. <https://doi.org/10.3208/jgssp.v08.c06>
- Liu DH, Sun J, Zhong DH, Song LG (2012) Compaction quality control of earth-rock dam construction using real-time field operation data. *J Constr Eng Manag* 138(9):1085–1094. [https://doi.org/10.1061/\(ASCE\)CO.1943-7862.0000510](https://doi.org/10.1061/(ASCE)CO.1943-7862.0000510)
- Zhang QL, Liu TY, Zhang ZS, Huangfu ZH, Li QB, An ZZ (2019) Compaction quality assessment of rockfill materials using roller-integrated acoustic wave detection technique. *Autom Constr* 97:110–121. <https://doi.org/10.1016/j.autcon.2018.11.003>
- Liu DH, Li ZL, Lian ZH (2014) Compaction quality assessment of earth-rock dam materials using roller-integrated compaction monitoring technology. *Autom Constr* 44:234–246. <https://doi.org/10.1016/j.autcon.2014.04.016>
- Hua TB, Yang ZH, Yang XG, Huang HC, Yao Q, Wu GJ, Li HT (2020) Assessment of geomaterial compaction using the pressure-wave fundamental frequency. *Transp Geotech* 22:100318. <https://doi.org/10.1016/j.trgeo.2020.100318>

13. Nie ZH, Jiao T, Wang X, Qiu T (2018) Assessment of compaction quality based on two index parameters from roller-integrated compaction measurements. *J Test Eval* 46(1):428–433. <https://doi.org/10.1520/JTE20150512>
14. Nie ZH, Wang X, Jiao T (2016) Anomalous data detection for roller-integrated compaction measurement. *Int J Geomech* 16(1):B4015004-1-B4015004-6. [https://doi.org/10.1061/\(ASCE\)GM.1943-5622.0000498](https://doi.org/10.1061/(ASCE)GM.1943-5622.0000498)
15. Zagyapan M, Fairfield CA (2002) Continuous surface wave and impact methods of measuring the stiffness and density of railway ballast. *NDT & E Int* 35(2):75–81. [https://doi.org/10.1016/S0963-8695\(01\)00034-2](https://doi.org/10.1016/S0963-8695(01)00034-2)
16. Zhang QL, An ZZ, Liu TY et al (2020) Intelligent rolling compaction system for earth-rock dams. *Autom Constr* 116:103246. <https://doi.org/10.1016/j.autcon.2020.103246>
17. Xu QW, Chang GK (2016) Adaptive quality control and acceptance of pavement material density for intelligent road construction. *Autom Constr* 62:78–88. <https://doi.org/10.1016/j.autcon.2015.11.004>
18. Liu DH, Lin M, Li S (2016) Real-time quality monitoring and control of highway compaction. *Autom Constr* 62:114–123. <https://doi.org/10.1016/j.autcon.2015.11.007>
19. White DJ, Jaselskis EJ, Schaefer VR (1936) Cackler ET (2005) Real-time compaction monitoring in cohesive soils from machine response. *Transp Res Rec* 1:172–180. <https://doi.org/10.1177/0361198105193600120>
20. Kumar SA, Aldouri R, Nazarian S, Si J (2016) Accelerated assessment of quality of compacted geomaterials with intelligent compaction technology. *Constr Build Mater* 113:824–834. <https://doi.org/10.1016/j.conbuildmat.2016.03.117>
21. Adam D. Continuous compaction control (CCC) with vibratory rollers (1997). In *Proceedings of the Australia-New Zealand Conference on Environmental Geotechnics-GeoEnvironment 97*. Melbourne, Victoria, Australia, A A Balkema, Brookfield, the Netherlands, pp 245–250.
22. Pistol J, Villwock S, Völkl W, Kopf F, Adam D (2016) Continuous compaction control (CCC) with oscillating rollers. *Procedia Eng* 143:514–521. <https://doi.org/10.1016/j.proeng.2016.06.065>
23. Meehan CL, Cacciola DV, Tehrani FS, Baker WJ III (2017) Assessing soil compaction using continuous compaction control and location-specific in situ tests. *Autom Constr* 73:31–44. <https://doi.org/10.1016/j.autcon.2016.08.017>
24. Zhang QL, Liu TY, Zhang ZS et al (2019) Unmanned rolling compaction system for rockfill materials. *Autom Constr* 100:103–117. <https://doi.org/10.1016/j.autcon.2019.01.004>
25. Bian YM, Yang M, Fang XJ, Wang XH (2017) Kinematics and path following control of an articulated drum roller. *Chin J Mech Eng* 30:888–899. <https://doi.org/10.1007/s10033-017-0102-8>
26. Yang M, Bian YM, Liu GJ, Zhang H (2020) Path tracking control of an articulated road roller with sideslip compensation. *IEEE Access* 8:127981–127992. <https://doi.org/10.1109/ACCESS.2020.3008455>
27. Guan SW, Wang JJ, Wang XL et al (2022) Dynamic hyperparameter turning-based path tracking control for robotic rollers working on earth-rock dam under complex construction conditions. *Autom Constr* 143:104576. <https://doi.org/10.1016/j.autcon.2022.104576>
28. An ZZ, Liu TY, Zhang ZS et al (2020) Dynamic optimization of compaction process for rockfill materials. *Autom Constr* 110:103038. <https://doi.org/10.1016/j.autcon.2019.103038>
29. Zhang QL, An ZZ, Liu TY et al (2020) Intelligent control theory of earth-rock dam compaction. *J Hydroele Eng* 39(7):34–40. <https://doi.org/10.11660/slfdbx.20200704>
30. Wang JJ, Qi NC, Zhong DH et al (2022) Development and application of native-integrated intelligent unmanned compaction system for high core rockfill dam. *J Hydraul Eng* 53(12):1421–1432. <https://doi.org/10.13243/j.cnki.slxb.20220253>
31. Xu GH (2019) The technology for continuous and intelligent compaction control of high-speed railway subgrade. China Railway Publishing House, Beijing, China, p 33
32. JT/T 3165-1993 (1993) Geotechnical density (filling sand method) tester technical conditions. Highway & Transportation Industry Standard
33. SL 237-004-1999 (1999) Specification of soil test. Ministry of Water Resources the People's Republic of China
34. Li XY, Wang S, Ruan JB (2004) Electromagnetic soil density measurement instrument. CN Patent CN2641654, China National Intellectual Property Administration
35. Tang X (2020) Nuclear density detector for roadbed filling materials in road engineering. CN Patent CN211263078U, China National Intellectual Property Administration
36. Li HF (2014). Soil non-nuclear density meter. CN Patent CN203502318U, China National Intellectual Property Administration
37. Refeai TA, Suhaibani AA (1997) Prediction of CBR using dynamic cone penetrometer. *J King Saud Univ Eng Sci* 9(2):191–203. [https://doi.org/10.1016/S1018-3639\(18\)30676-7](https://doi.org/10.1016/S1018-3639(18)30676-7)
38. Clegg B (1980). An impact soil test as alternative to California bearing ratio. In *Proceedings of the 3<sup>rd</sup> ANZ Geomechanics Conference, Vol. 1*, Wellington, New Zealand, pp 225–230. [https://doi.org/10.1016/0148-9062\(82\)90255-8](https://doi.org/10.1016/0148-9062(82)90255-8)
39. Shabbir HM, Apegyei A (2010) Evaluation of the lightweight deflectionometer for in-situ determination of pavement layer moduli. Virginia Transportation Research Council, Charlottesville, VA, US
40. Elhakim AF, Elbaz K, Amer MI (2014) The use of a lightweight deflectionometer for in situ evaluation of the sand degree of compaction. *HBRC J* 10(3):298–307. <https://doi.org/10.1016/j.hbrj.2013.12.003>
41. Lee CH, Kim KS, Woo W, Lee W (2014) Soil stiffness gauge (SSG) and dynamic cone penetrometer (DCP) tests for estimating engineering properties of weathered sandy soils in Korea. *Eng Geol* 169:91–99. <https://doi.org/10.1016/j.enggeo.2013.11.010>
42. Andersen KH, Stenhamar P (1982) Static plate loading tests on overconsolidated clay. *J Geotech Eng Div* 108(7):918–934. <https://doi.org/10.1061/AJGEB6.0001315>
43. Huang SX, Liu JN, Wu XM (2005) GPS real-time supervisory system and its preliminary application in the construction of face rockfill dam. *Geomat Inform Sci Wuhan Univ* 30(9):813–816
44. Oloufa AA (2002) Quality control of asphalt compaction using GPS-based system architecture. *IEEE Robot Autom Mag* 9(1):29–35. <https://doi.org/10.1109/100.993152>
45. Zhong DH, Liu DH, Cui B (2011) Real-time compaction quality monitoring of high core rockfill dam. *Sci China Tech Sci* 54(7):1906–1913. <https://doi.org/10.1007/s11431-011-4429-6>
46. Zhong DH, Liu DH, Cui B (2011) Real-time monitoring technology and application of compaction quality for high core wall rockfill dams. *Sci. Sin. Technol.* 41(08):1027–1034
47. Yao YP, Ruan YZ, Liu BY, Chen J, Jiang HX (2015) Control technology of construction quality for high filled airports based on Beidou satellite navigation system. *Chin J Geotech Eng* 37(S2):6–10
48. Huang SX, Zhang W, Wu G (2018) Research on real-time supervisory system for compaction quality in face rockfill dam engineering. *J Sens* 2018:1–11. <https://doi.org/10.1155/2018/6487405>
49. Ma HQ, Zhong DH, Zhang ZL, Sun YJ, Liu DH (2011) Key technologies of real-time construction control for major hydraulic and hydroelectric projects. *Strategic Study of CAE* 13(12):20–27
50. Lin ED (2015) Research and application of a new generation of compaction construction quality monitoring system. In *Proceedings of Technical Progress of Hydropower Sustainable Development and Roller Compacted Concrete Dam Construction: 2015 annual academic conference of China Dam Association, Yellow River Water Conservancy Press*, pp 527–534 (in Chinese)
51. Dynapac Maskin AB (1981) Guidelines for the use of the compactometer. Swedish National Road and Transport Research Institute, Monograph, Sweden
52. Li YY, Li ZG, Ma ZX, et al. (2021) A method of continuous compaction control for rockfill dams. CN Patent CN112647387A, China National Intellectual Property Administration.
53. Xu GH, Luo ZH, Tian B (2015) A review of the development of continuous compaction control technology. *Road Mach Constr Mech* 32(8):34–38
54. Ma Y, Zhang Y, Zhao W et al (2022) Assessment of intelligent compaction quality evaluation index and uniformity. *J Transp Eng Part B Pavements* 148(2):04022024. <https://doi.org/10.1061/JPEODX.0000368>
55. Wang N, Ma T, Chen F, Ma Y (2022) Compaction quality assessment of cement stabilized gravel using intelligent compaction technology—A case study. *Constr Build Mater* 345:128100. <https://doi.org/10.1016/j.conbuildmat.2022.128100>

56. Hua TB, Yang XG, Yao Q, Li HT (2018) Assessment of real-time compaction quality test indexes for rockfill material based on roller vibratory acceleration analysis. *Adv Mater Sci Eng* 2018:1–15. <https://doi.org/10.1155/2018/2879321>
57. Thurner H, Sandström A (1980) A new device for instant compaction control. In Proceedings of the International Conference on Compaction. CiNii Articles, Paris, France, pp 611–614.
58. Scherocman JA, Rakowski S, Uchiyama K (2007) Intelligent compaction, does it exist? In Proceeding of the 52nd Annual Conference—Canadian Technical Asphalt Association. Niagara Falls, Canada, pp 1–25
59. Rinehart RV, Mooney MA (2008) Instrumentation of a roller compactor to monitor vibration behavior during earthwork compaction. *Autom Constr* 17(2):144–150. <https://doi.org/10.1016/j.autcon.2006.12.006>
60. Mooney MA, Rinehart RV (2007) Field monitoring of roller vibration during compaction of subgrade soil. *J Geotech Geoenviron Eng* 133(3):257–265. [https://doi.org/10.1061/\(ASCE\)1090-0241\(2007\)133:3\(257\)](https://doi.org/10.1061/(ASCE)1090-0241(2007)133:3(257))
61. Mooney MA, Gorman PB, Gonzalez JN (2005) Vibration-based health monitoring of earth structures. *Struct Health Monit* 4(2):137–152. <https://doi.org/10.1177/1475921705049759>
62. Vennapusa PKR, White DJ, Morris MD (2010) Geostatistical analysis for spatially referenced roller-integrated compaction measurements. *J Geotech Geoenviron Eng* 136(6):813–822. [https://doi.org/10.1061/\(ASCE\)GT.1943-5606.0000285](https://doi.org/10.1061/(ASCE)GT.1943-5606.0000285)
63. Thurner HF, Sandström ÅKE (2000) Continuous compaction control, CCC. In Proceedings of the European Workshop Compaction of Soils and Granular Materials. Paris, France, European Workshop Compaction of soils and Granular Materials, pp 237–246
64. Furuya H, Fujiyama T (2011) Development of soil stiffness evaluation equipment alfa-system using acceleration response of vibratory roller. In Proceedings of the 28th International Symposium on Automation and Robotics in Construction, Seoul, pp 337–342
65. Ling JM, Lin S, Qian JS et al (2018) Continuous compaction control technology for granite residual subgrade compaction. *J Mater Civil Eng* 30(12):04018316:1-04018316:9. [https://doi.org/10.1061/\(ASCE\)MT.1943-5533.0002522](https://doi.org/10.1061/(ASCE)MT.1943-5533.0002522)
66. Xu TY, Zhou ZJ, Yan RP et al (2020) Real-time monitoring method for layered compaction quality of loess subgrade based on hydraulic compactor reinforcement. *Sensors* 20(15):4288. <https://doi.org/10.3390/s20154288>
67. Shi MN, Wang JJ, Guan T et al (2022) Effective compaction power index for real-time compaction quality assessment of coarse-grained geomaterials: Proposal and comparative study. *Constr Build Mater* 321:126375. <https://doi.org/10.1016/j.conbuildmat.2022.126375>
68. Heng RBW, Nor MJM (1998) Statistical analysis of sound and vibration signals for monitoring rolling element bearing condition. *Appl Acoust* 53(1–3):211–226. [https://doi.org/10.1016/S0003-682X\(97\)00018-2](https://doi.org/10.1016/S0003-682X(97)00018-2)
69. Ilori AO, Okwueze EE, Obianwu VI (2013) Evaluating compaction quality using elastic seismic p wave. *J Mater Civil Eng* 25(6):693–700. [https://doi.org/10.1061/\(ASCE\)MT.1943-5533.0000559](https://doi.org/10.1061/(ASCE)MT.1943-5533.0000559)
70. Kim DS, Shin MK, Park HC (2001) Evaluation of density in layer compaction using SASW method. *Soil Dyn Earthq Eng* 21(1):39–46. [https://doi.org/10.1016/S0267-7261\(00\)00076-2](https://doi.org/10.1016/S0267-7261(00)00076-2)
71. DalMoro G, Al-Arif N, Moustafa SSR (2016) Assessing ground compaction via time lapse surface wave analysis. *Acta Geodynamic Et Geomaterialia* 13(3):249–256. <https://doi.org/10.13168/AGG.2016.0006>
72. Zhang HC, Dai JL, Li XZ (2007) Compactness automatic detecting method of subgrade for intelligent impact roller. *J Traffic Transp Eng* 7(5):63–67
73. Thompson MJ, White DJ (2008) Estimating compaction of cohesive soils from machine drive power. *J Geotech Geoenviron Eng* 134(12):1771–1777. [https://doi.org/10.1061/\(ASCE\)1090-0241\(2008\)134:12\(1771\)](https://doi.org/10.1061/(ASCE)1090-0241(2008)134:12(1771))
74. Pistol J, Adam D (2018) Fundamentals of roller integrated compaction control for oscillatory rollers and comparison with conventional testing methods. *Transp Geotech* 17(Part B):75–84. <https://doi.org/10.1016/j.trgeo.2018.09.010>
75. Anderegg R, Kaufmann K (2004) Intelligent compaction with vibratory rollers: feedback control systems in automatic compaction and compaction control. *Transp Res Rec* 1868(1):124–134. <https://doi.org/10.3141/1868-13>
76. Xu GH, Gao H, Luo ZH et al (2017) Application of continuous and intelligent compaction control technology in high-speed railway construction. *Road Mach Constr Mech* 34(1):30–34
77. Liu DH, Gao L (2018) Analysis and improvement of roller vibration behavior-based indexes for monitoring compaction quality of earth-rock dams. *J Hydrol Eng* 37(4):111–120
78. Cheng LL, Zhou C, Lu J et al (2021) Nondestructive testing method of compactness quality for airport subgrade based on ground penetrating radar. *Constr Technol* 50(14):98–101
79. Brandl H, Adam D (1997) Sophisticated continuous compaction control of soils and granular materials. In Proceedings of 14<sup>th</sup> International Conference on Soil Mechanics and Foundation Engineering, International Society for Soil Mechanics and Geotechnical Engineering, Hamburg, pp 31–36
80. Ye YS, Cai DG, Zhu HW et al (2020) Research on new continuous compaction control index of high-speed railway subgrade based on vibration energy. *J China Railway Soc* 42(7):127–132
81. Wu LL (2020) Research on continuous compaction control technology of roadbed based on energy dissipation. Dissertation, China Academy of Railway Sciences, China
82. Liu DH, Li ZL, Wang AG (2014) Roller working-based real-time monitoring and rapid assessment of rock-fill dam compaction quality. *J Hydraul Eng* 45(10):1223–1230. <https://doi.org/10.13243/j.cnki.slxb.2014.10.011> (in Chinese)
83. Xu GH, Gao H, Wang ZR (2007) Continuous dynamic monitor technology on subgrade compaction quality. *Chin J Highway Trans* 20(3):17–22. <https://doi.org/10.19721/j.cnki.1001-7372.2007.03.004>
84. Liu DH, Wang GF (2010) Compaction quality evaluation of the entire rolled unit of earth dam based on real-time monitoring. *J Hydraul Eng* 41(6):720–726, (in Chinese) <https://doi.org/10.13243/j.cnki.slxb.2010.06.010>
85. Wang XL, Zhou L, Ren BY et al (2015) Dual evaluation on rolling compaction quality of rock-fill dam based on real-time monitoring. *J Hydroel Eng* 34(2):164–170
86. Wang F, Zhong DH, Yan YL et al (2018) Rockfill dam compaction quality evaluation based on cloud-fuzzy model. *J Zhejiang Univ-Sci A (Appl Phys & Eng)* 19(4):289–303. <https://doi.org/10.1631/jzus.A1600753>
87. An ZZ, Liu TY, HuangFu ZH et al (2020) Neural network model for evaluating compaction quality of rockfill materials by compaction meter value. *J Hydroel Eng* 39(4):110–120
88. Wang JJ, Zhong DH, Wu BP, Shi MN (2018) Evaluation of compaction quality based on SVR with CFA: case study on compaction quality of earth-rock dam. *J Comput Civ Eng* 32(3):05018001. [https://doi.org/10.1061/\(ASCE\)CP.1943-5487.0000742](https://doi.org/10.1061/(ASCE)CP.1943-5487.0000742)
89. Wang JJ, Zhong DH, Adeli H, Wang D, Liu MH (2018) Smart bacteria-foraging algorithm-based customized kernel support vector regression and enhanced probabilistic neural network for compaction quality assessment and control of earth-rock dam. *Expert Systems* 35:e12357. <https://doi.org/10.1111/exsy.12357>
90. Wang JJ, Zhong DH, Wang F (2016) Evaluation of compaction quality of earth-rock dam based on bacterial foraging support vector regression algorithm. In Proceedings of the International Conference on Innovative Material Science and Technology (IMST 2016). Shenzhen, China, Atlantis Press, pp 265–270
91. Hong Y, Tian ZH, Sun X (2020) Dynamic evaluation for compaction quality of roller compacted concrete based on reliability metrics. *J Constr Eng Manag* 146(10):04020123. [https://doi.org/10.1061/\(ASCE\)CO.1943-7862.0001925](https://doi.org/10.1061/(ASCE)CO.1943-7862.0001925)
92. Liu DH, WY (2019) Fuzzy comprehensive evaluation of earth-rock dam compaction quality based on real-time monitoring. *J Hydroelectr Eng* 38(3):142–153
93. Wu LL, Jiang HH, Tand JW et al (2020) Continuous compaction monitoring technology based on multiple regression analysis. *Rock Soil Mech* 41(6):2081–2090. <https://doi.org/10.16285/j.rsm.2019.1.291>
94. Hua TB, Yang ZH, Yang XG et al (2020) Assessment of geomaterial compaction using the pressure-wave fundamental frequency. *Transp Geotech* 22:100318. <https://doi.org/10.1016/j.trgeo.2020.100318>
95. Liu DH, Wang AG, Liu YG, Li BY (2014) Real-time monitoring and assessment of compaction quality for earth-rock dam basing on roller vibration behavior analysis. *J Hydraul Eng* 45(2):163–170. <https://doi.org/10.13243/j.cnki.slxb.2014.02.005>

96. Cui B, Zhang HG, Wang JJ, Yu J (2021) Real time evaluation of compaction quality of gravelly soil core wall based on construction process parameters. *Water Resour Hydropower Eng* 52(2):109–118. <https://doi.org/10.13928/j.cnki.wrahe.2021.02.012>
97. Sun M (1985) Automatic control device and rolling driving method of Japanese road rolling machinery. *Road Mach Constr Mech* 2:34–37
98. Liu TY, Li QB, Fang K (2015) Automatic driving system and method for hydraulic construction vibratory rolling machine. CN Patent CN105137997A, China National Intellectual Property Administration
99. Liu TY, Zhang QL, Li YD et al. (2015) An intelligent rolling robot. CN Patent CN105002810A, Beijing, China National Intellectual Property Administration
100. Zhang QL, Liu TY, Li QB et al (2018) Automatic rolling system based on closed-loop feedback control and RTK-GPS. *J Hydroelectr Eng* 37(5):151–160
101. Cui B, Li SP, Tang MY et al. (2018) An automatic driving system for rollers. CN Patent CN108691309A, China National Intellectual Property Administration
102. Zhong DH, Shi MN, Cui B et al. (2018) An unmanned method of vibratory rolling machine applied to the construction of water conservancy projects. CN Patent CN10879277A, China National Intellectual Property Administration
103. Yu GZ, Wu JX, Wang YP et al. (2016) A steering control mechanism for automatic vehicle driving. CN Patent CN105547710A, China National Intellectual Property Administration
104. Luo XQ, Bi JF (2018) Unmanned intelligent vibration roller and system for earthwork engineering. CN Patent CN107761701A, China National Intellectual Property Administration
105. Gao Y, Yang M, Jia YS (2019) Laser-assisted positioning system for driverless road rollers driving in a straight line. CN Patent CN110568844A, China National Intellectual Property Administration
106. Bian YM, Fang XJ, Yang M et al (2017) Automatic rolling control for unmanned vibratory roller based on fuzzy algorithm. *J Tongji Univ (Nat Sci)* 45(12):1830–1838
107. Dai L, Zhai YM, Qin W (2019) Unmanned rollers. CN Patent CN109162174A, China National Intellectual Property Administration
108. Chen ZY, Zhao YF, Zou B et al (2019) Study and application of unmanned driving technology or filling and rolling construction of earth-rockfill dam. *Water Resour Hydropower Eng* 50(8):1–7. <https://doi.org/10.13928/j.cnki.wrahe.2019.08.001>
109. Ye YS, Cai DG, Zhu HW et al. (2019) Intelligent compaction system for subgrade based on unmanned and information-based detection technology. CN Patent CN109898391A, China National Intellectual Property Administration
110. Feng JW (2000) China's first unmanned road roller on the road in style. *China Mach Electric Ind* 24:17
111. He PC, Wu GJ, Zhang HT et al. (2016) An automatic operating system for vibration rollers and its usage method. CN Patent CN105887627A, China National Intellectual Property Administration
112. Huang WZ, Wang D, Xiao ZD et al (2020) Design and implementation of PLC-based autonomous construction system of unmanned vibratory roller. *Comput. Mater. Contin.* 65:897–912. <https://doi.org/10.32604/cmc.2020.09728>
113. Li QY, Liu TY, Luo DG et al. (2020) An unmanned roller compaction system. CN Patent CN211340302U, China National Intellectual Property Administration
114. Yao DC, Xie H, Qiang W et al (2018) Accurate trajectory tracking with disturbance-resistant and heading estimation method for self-driving vibratory roller. *IFAC-PaperOnLine* 51(31):754–758. <https://doi.org/10.1016/j.ifacol.2018.10.135>
115. Song K, Xie H (2020) Path-following control for unmanned rollers: a composite disturbance rejection-based framework. In *Proceedings of the 2020 IEEE 9<sup>th</sup> Data Driven Control and Learning Systems Conference*. IEEE, Liuzhou, China, pp 432–437
116. Fang XJ, Bian YM, Yang M et al (2018) Development of a path following control model for an unmanned vibratory roller in vibration compaction. *Adv Mech Eng* 10(5):1–16. <https://doi.org/10.1177/1687814018773660>
117. Song EB, Yao YP (2023) Method of improving tracking precision of planning path for impact rollers. *J Beijing Univ. Aeronaut Astronaut (Nat Sci)* 49(1):106–114. <https://doi.org/10.13700/j.bh.1001-5965.2021.0495>
118. Zhang H, Wang CE, Pan WG et al. (2019) Automatic driving control system for impact roller. CN Patent CN209343201U
119. Shi MN, Cui B, Wang JJ et al (2020) Research on cooperative complete coverage path planning for unmanned roller group under complex construction conditions. *J Hydraul Eng* 51(12):1544–1557
120. Shi MN, Wang JJ, Li QH et al (2022) Accelerated earth-rockfill dam compaction by collaborative operation of unmanned roller fleet. *J Constr Eng Manag* 148(7):04022046. [https://doi.org/10.1061/\(ASCE\)CO.1943-7862.0002267](https://doi.org/10.1061/(ASCE)CO.1943-7862.0002267)
121. Tsinghua Water Conservancy Department (2020) The construction of the world's first unmanned highway roller fleet has started, and the Tsinghua team has assisted in completing intelligent construction during the epidemic period. <https://www.civil.tsinghua.edu.cn/he/info/1043/1293.htm>. Accessed 31 May 2020
122. Wu JJ, Liu YC, Xia YQ (2020) XCMG's driverless equipment shines in Jingxiang-An unmanned cluster intelligent construction observation meeting for the pavement project of Jingxiang Expressway. *Munic Eng Technol* 38(6):4–6
123. China Construction Machinery Trading Network (2021) Multi-scene, all working conditions! Sany's unmanned road fleet is installed on a large scale in China. <https://www.163.com/dy/article/G8H2CU090518VM2A.html>. Accessed 26 April 2021
124. Botev V, Azidhak A (2015) Intelligent compaction-autonomous compactor concept evaluation. Dissertation, University of Gothenburg
125. Lin MS, Wang GY (2021) An intelligent rolling system for subgrade and pavement. CN Patent CN109356003B, China National Intellectual Property Administration
126. Yao YP, Song EB (2023) Research on real-time quality evaluation method for intelligent compaction of soil-filling. *Transp Geotech* 39:100943. <https://doi.org/10.1016/j.tgeo.2023.100943>
127. Ma Y, Chen F, Ma T et al (2021) Intelligent compaction: an improved quality monitoring and control of asphalt pavement construction technology. *IEEE Trans Intell Transp Syst* 23(9):14875–14882. <https://doi.org/10.1109/TITS.2021.3134699>
128. Ruan YZ (2018) A real-time monitoring system for compaction of high embankment in airport engineering based on cloud radiation. Dissertation, Beihang University (in Chinese)

## Publisher's Note

Springer Nature remains neutral with regard to jurisdictional claims in published maps and institutional affiliations.